

# PURIFICATION BEFORE FUSION: TOWARD MASK-FREE SPEECH ENHANCEMENT FOR ROBUST AUDIO-VISUAL SPEECH RECOGNITION

*Linzhi Wu<sup>1,2</sup>, Xingyu Zhang<sup>2\*</sup>, Hao Yuan<sup>3,2</sup>, Yakun Zhang<sup>2</sup>, Changyan Zheng<sup>4,2</sup>  
 Liang Xie<sup>2</sup>, Tiejun Liu<sup>1</sup>, Erwei Yin<sup>2</sup>*

<sup>1</sup>University of Electronic Science and Technology of China, Chengdu, China

<sup>2</sup>Defense Innovation Institute, Academy of Military Sciences, Beijing, China

<sup>3</sup>Peking University, Beijing, China

<sup>4</sup>High-tech Institute, Weifang, China

## ABSTRACT

Audio-visual speech recognition (AVSR) typically improves recognition accuracy in noisy environments by integrating noise-immune visual cues with audio signals. Nevertheless, high-noise audio inputs are prone to introducing adverse interference into the feature fusion process. To mitigate this, recent AVSR methods often adopt mask-based strategies to filter audio noise during feature interaction and fusion, yet such methods risk discarding semantically relevant information alongside noise. In this work, we propose an end-to-end noise-robust AVSR framework coupled with speech enhancement, eliminating the need for explicit noise mask generation. This framework leverages a Conformer-based bottleneck fusion module to implicitly refine noisy audio features with video assistance. By reducing modality redundancy and enhancing inter-modal interactions, our method preserves speech semantic integrity to achieve robust recognition performance. Experimental evaluations on the public LRS3 benchmark suggest that our method outperforms prior advanced mask-based baselines under noisy conditions.

**Index Terms**— audio-visual speech recognition, speech feature enhancement, noise-robust, multimodal bottleneck Conformer

## 1. INTRODUCTION

Audio-visual speech recognition (AVSR) has emerged as a promising solution to overcome the limitations of automatic speech recognition (ASR) systems, especially in noisy conditions. By incorporating visual cues such as lip movements, AVSR leverages complementary multimodal information to improve recognition robustness, attracting considerable attention recently [1, 2, 3]. Unlike audio-only ASR, which struggles with degraded performance under challenging acoustic conditions, AVSR exploits visual modality to provide contextual cues that are invariant to acoustic noise, thereby enabling reliable speech transcription even in scenarios with background noise or overlapping speech [4, 5].

Most contemporary AVSR models employ cross-modal attention mechanisms to facilitate effective audio-visual interaction [6, 7, 8, 9, 10]. Compared to early strategies such as direct feature concatenation, cross-attention achieves dynamic alignment and

richer multimodal integration. But, when audio inputs are severely corrupted by noise, the interaction process is prone to disruption. Noisy audio features can introduce irrelevant or misleading information, forcing the model to undertake the entangled tasks of both implicitly “denoising” the input and “extracting” critical speech-related information simultaneously. This dual burden might overwhelm the cross-modal interaction module, leading to suboptimal feature fusion. To alleviate the negative effects of noise, recent studies have proposed custom-designed masking networks to generate noise-reduction masks, which explicitly suppress irrelevant noise components in audio features [4, 11, 12]. These methods aim to suppress noise by selectively focusing on relevant audio information during fusion. Nevertheless, they are typically driven solely by the final AVSR objective, which cannot guarantee the preservation of semantic integrity during this lossy noise-suppression process.

By contrast, this work presents a purify-then-fuse paradigm without explicit mask generation to achieve noise-robust AVSR. The key insight is that prioritizing feature purification before fusion ensures that audio representations fed into cross-modal interaction are semantically complete and noise-free. To this end, we incorporate an auxiliary audio-visual speech enhancement module based on bottleneck attention into our AVSR framework, which refines audio representations prior to deep multimodal fusion. Motivated by [13], we design an audio-visual bottleneck Conformer to facilitate efficient cross-modal interaction and implicit noise purification. Guided by audio spectrogram reconstruction objectives, our model tries to extract robust and semantically rich audio representations with the aid of visual cues, mitigating noise interference while retaining essential speech information. To our knowledge, this is the first attempt to exploit a multimodal bottleneck Conformer for both efficient cross-modal interaction and reconstruction-based constraints, thus enhancing model resilience to noise. We evaluate the effectiveness of the proposed method through a series of experiments on LRS3 [14], the large-scale audio-visual dataset obtained in the wild. The results demonstrate that our model achieves superior performance over previous competitive methods, confirming its robustness under challenging acoustic conditions.

## 2. PROPOSED METHOD

Fig. 1 illustrates the proposed noise-robust AVSR framework, which processes video and noisy audio inputs to achieve speech recognition without relying on explicit masks. The framework integrates a primary AVSR model with a dedicated speech enhancement (de-

\*Corresponding author. This work was supported in part by the grants from the National Natural Science Foundation of China under Grant 62332019, the National Key Research and Development Program of China (2023YFF1203900, 2023YFF1203903), and sponsored by Beijing Nova Program (20240484513).

noising) module that reconstructs cleaner audio representations. The enhancement module is placed after audio feature extraction and before cross-modal fusion, and it is jointly trained end-to-end with the AVSR model. The refined audio features are then passed through a cross-modal encoder and fused with the visual features, enabling deeper and more reliable speech understanding.

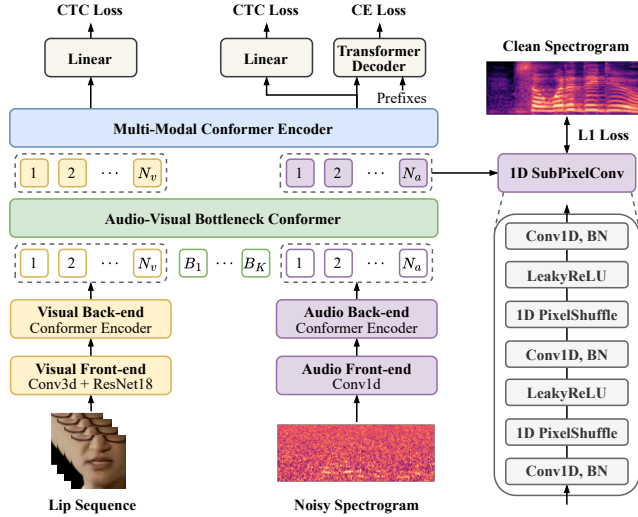


**Fig. 1.** Overall architecture of the proposed model.

## 2.1. Feature Extraction

The video input, denoted as  $\mathbf{x}_v$ , consists of mouth region-of-interest (RoI) sequences. These are first processed by a 3D convolutional layer with a kernel size of  $5 \times 7 \times 7$  followed by a 2D ResNet18 [15] to extract spatio-temporal features. The resulting features are then fed into a three-layer Conformer encoder [16], which captures both local and global visual temporal dynamics, yielding visual features  $\mathbf{h}_v \in \mathbb{R}^{N_v \times d}$ . The audio input, denoted as log mel-spectrogram  $\mathbf{x}_a$ , is first processed by two subsampling 1D convolutional layers to reduce the temporal dimension to match the frame rate of the visual features. A similar Conformer is then applied to encode temporal features, producing audio features  $\mathbf{h}_a \in \mathbb{R}^{N_a \times d}$ . Here  $N_v$  and  $N_a$  are total frames of video and audio respectively, and  $d$  is the feature dimension. Each modality frame refers to a token in our work.

## 2.2. Audio-Visual Bottleneck Conformer

To enhance inter-modal interaction and compress redundant modal information, we introduce an audio-visual bottleneck Conformer (AVBC) with  $L$  layers, inspired by [13]. The AVBC employs a small set of learnable bottleneck tokens  $\mathbf{b}^0 = [b_1, b_2, \dots, b_K]$ ,  $b_i \in \mathbb{R}^d$  ( $K \ll N_a, N_v$ ). For each modality, cross-attention is computed between its feature sequence and the bottleneck tokens. Formally for layer  $l$ , we calculate token representations as follows:

$$\begin{aligned} \mathbf{h}_v^{l+1} \parallel \mathbf{b}_v^{l+1} &= \text{Conformer}(\mathbf{h}_v^l \parallel \mathbf{b}^l; \theta_v), \\ \mathbf{h}_a^{l+1} \parallel \mathbf{b}_a^{l+1} &= \text{Conformer}(\mathbf{h}_a^l \parallel \mathbf{b}^l; \theta_a), \\ \mathbf{b}^{l+1} &= (\mathbf{b}_v^{l+1} + \mathbf{b}_a^{l+1})/2, \end{aligned} \quad (1)$$

where  $\theta_v$  and  $\theta_a$  are the parameters of the visual Conformer and the audio Conformer, respectively. “ $\parallel$ ” denotes the concatenation oper-

ation of the latent tokens. Note that the convolution module within the Conformer block is only used for modality tokens excluding the bottleneck tokens. The iterative bottleneck attention computation across  $\mathbf{h}_a$  and  $\mathbf{h}_v$  ultimately yields compressed representations  $\mathbf{z}_v = \mathbf{h}_v^L$  and  $\mathbf{z}_a = \mathbf{h}_a^L$ . Since all cross-modal attention flow must pass through these bottleneck tokens, such tight “fusion” bottlenecks force the model to condense modality-specific information and share only essential content. This design allows the visual modality to guide the purification of noisy audio features in a computationally efficient manner, which reduces cross-modal attention computations from  $\mathcal{O}((N_a + N_v)^2)$  to  $\mathcal{O}((K + N_a)^2) + \mathcal{O}((K + N_v)^2)$ .

## 2.3. Speech Feature Enhancement

To refine noisy audio features into fusion-ready representations, we reconstruct the clean mel-spectrogram  $\hat{\mathbf{x}}_a$  from  $\mathbf{z}_a$  via a dedicated 1D sub-pixel convolution layer [17], which efficiently up-scales audio feature maps to produce the final spectrogram output<sup>1</sup>. The reconstruction loss is defined as the L1 distance between the mel-spectrogram of the clean audio and the reconstructed mel-spectrogram:

$$\mathcal{L}_{\text{recon}} = \|\hat{\mathbf{x}}_a - \mathbf{x}_a^{\text{clean}}\|_1, \quad (2)$$

Inspired by the perceptual loss used for image processing [18], we further introduce a spectrogram-based perceptual loss. Unlike reconstruction loss, which only focuses on raw spectrogram similarity, this loss function captures perceptual discrepancies by minimizing the L2 distance between high-level feature maps of the target and reconstructed mel-spectrograms, where the feature maps are typically obtained by an optimized feature extractor:

$$\mathcal{L}_{\text{percep}} = \|\mathcal{F}(\hat{\mathbf{x}}_a) - \mathcal{F}(\mathbf{x}_a^{\text{clean}})\|_2^2, \quad (3)$$

where  $\mathcal{F}$  is our custom audio front-end in our work, achieving a cycle-consistency regularization. The whole speech feature enhancement process is guided by these two loss functions:

$$\mathcal{L}_{\text{enhance}} = \alpha_1 \mathcal{L}_{\text{recon}} + \alpha_2 \mathcal{L}_{\text{percep}}, \quad (4)$$

with the first loss term providing stability (avoid drift in scale) and the second one driving speech intelligibility.  $\alpha_1$  and  $\alpha_2$  denote the weighting factors for each loss term.

## 2.4. Fusion and Speech Recognition

The cross-modal fusion encoder is not required to dedicate substantial effort to denoising; instead, its primary role focuses on integrating the purified audio with visual information. The refined representations  $\mathbf{z}_v$  and  $\mathbf{z}_a$  are concatenated along the temporal dimension and processed by a Conformer encoder to fully capture intra-modal and inter-modal temporal dependencies [9], yielding fused features  $\mathbf{f}_v$  and  $\mathbf{f}_a$  as follows:

$$\mathbf{f}_a \parallel \mathbf{f}_v = \text{Conformer}(\mathbf{z}_a \parallel \mathbf{z}_v; \theta_f), \quad (5)$$

where  $\theta_f$  is the encoder parameter. These are fed into the CTC [19] projection layer and Transformer decoder [20] for speech recognition. Given the target text sequence  $\mathbf{y}$ , the recognition objective

<sup>1</sup>For the spectrogram decoder, our preliminary experiments have shown that the designed lightweight sub-pixel convolution module delivers performance comparable to the widely-used transposed convolution network, while requiring fewer parameters and offering higher computational efficiency.

function is defined as a hybrid CTC/attention loss [21, 22]:

$$\begin{aligned}\mathcal{L}_{AVSR} &= \lambda \mathcal{L}_{ctc} + (1 - \lambda) \mathcal{L}_{att}, \\ \mathcal{L}_{ctc} &= -\log p_{ctc}(\mathbf{y}|\mathbf{f}_v) - \log p_{ctc}(\mathbf{y}|\mathbf{f}_a), \\ \mathcal{L}_{att} &= -\log p_{att}(\mathbf{y}|\mathbf{f}_a),\end{aligned}\quad (6)$$

where  $\lambda$  balances the relative weight between the CTC and cross-entropy attention-based losses. The CTC projection layer is shared across modalities.

The overall optimization objective combines recognition and enhancement losses:  $\mathcal{L}_{\text{total}} = \mathcal{L}_{AVSR} + \mathcal{L}_{\text{enhance}}$ . This speech enhancement module is jointly trained with the AVSR modules. Accordingly, the loss function backpropagates through the enhancement module, compelling it to produce audio representations that are optimal for speech transcription, not merely for spectral fidelity.

### 3. EXPERIMENTS

#### 3.1. Data Processing

**Dataset.** We evaluate the proposed method on the large-scale audio-visual benchmark LRS3 [14], which consists of about 439 hours of TED and TEDx English talks sourced from YouTube<sup>2</sup>. The training set is divided into two partitions: *pretrain* (408 hours) and *trainval* (30 hours), both of which are transcribed at the sentence level. The *pretrain* part differs from *trainval* in that the duration of its video clips span a much broader range. The standard *test* set (0.9 hours) is used for evaluation.

**Processing.** For the video stream, mouth RoIs are cropped from the aligned talking face video sequence at 25Hz, resized to  $96 \times 96$ , converted to grayscale, and normalized to  $[0, 1]$ . During training, we apply random cropping with crop size  $88 \times 88$ , horizontal flipping (probability 0.5) and adaptive time masking [23] to augment the video data. We apply center crop at inference time. For the audio stream, raw waveforms are resampled at 16kHz and transformed into 80-dimensional log mel-spectrograms over windows of 25 ms strided by 10 ms. To synthesize noisy audio inputs for training, we select white, pink, factory1, factory2 and babble noises from the NOISEX-92 database [24], and extract additional overlapping speech noise samples from the training data. These noise samples are then additively mixed with clean waveforms at a signal-to-noise ratio (SNR) level in  $\{-7.5, -2.5, 2.5, 7.5, 12.5, 17.5\}$  dB. For each training sample, we uniformly randomly select either a clean or noisy speech.

#### 3.2. Experimental Settings

**Model Setup.** Each Conformer encoder within our framework for each modality consists of 3 blocks with 4 attention heads, hidden dimensions of 512, feed-forward dimensions of 2048, and a convolution kernel size of 31. We leverage a standard Transformer decoder for prediction and the decoder comprises 6 layers, 4 attention heads, hidden dimensions of 512, and feed-forward dimensions of 2048. Following [2, 12], the visual front-end is initialized using a pre-trained model on LRW [25]. The learnable bottleneck tokens are initialized using a Gaussian with a mean of 0 and a standard deviation of 0.02, and the number of tokens is set to 4.

**Training Setup.** We use the AdamW optimizer [26] to update model parameters for 70 epochs with a batch size of 16. The initial learning rate is set to 0.001, adjusted by a cosine annealing schedule with a linear warm-up.  $\lambda$  is set to 0.1 as suggested in [23], and  $\alpha_1 = \alpha_2 =$

<sup>2</sup>[https://www.robots.ox.ac.uk/~vgg/data/lip\\_reading/lrs3.html](https://www.robots.ox.ac.uk/~vgg/data/lip_reading/lrs3.html)

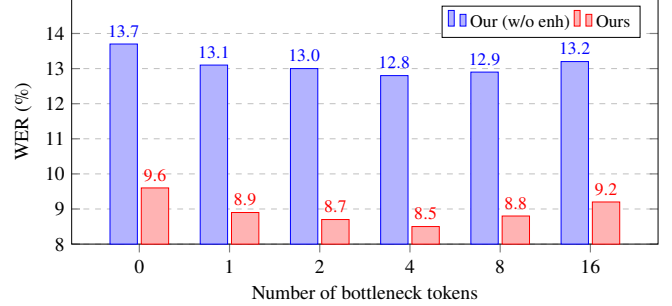


**Fig. 2.** Performance comparison of different token numbers at the first layer of our bottleneck Conformer under -5dB SNR babble noise. “w/o enh” indicates the model without speech enhancement.

**Table 1.** Effects of the reconstruction loss ( $\mathcal{L}_{\text{recon}}$ ) and the cycle-consistency loss ( $\mathcal{L}_{\text{percep}}$ ) on WER, where  $\mathcal{L}_{\text{percep}}$  is applied to the audio front-end and a pre-trained Whisper encoder, respectively.

Baseline	$\mathcal{L}_{\text{recon}}$	$\mathcal{L}_{\text{percep}}$ (Audio front-end)	WER (%)
✓	–	–	12.8
✓	✓	–	11.2
✓	–	✓	10.8
✓	✓	✓	<b>8.5</b>

Baseline	$\mathcal{L}_{\text{recon}}$	$\mathcal{L}_{\text{percep}}$ (Whisper)	WER (%)
✓	–	–	12.8
✓	✓	–	11.2
✓	–	✓	9.5
✓	✓	✓	<b>7.9</b>

0.1 in our work. For the training stability of the entire framework, we adopt a curriculum learning strategy. We first train the model for 20 epochs with the primary AVSR objective using relatively high SNRs (*i.e.*, 7.5-17.5dB), which focuses on establishing robust multimodal alignments and avoids early divergence induced by high-noise inputs. Then, we extend training to the full SNR range and incorporate auxiliary speech enhancement objectives for joint learning, enabling refined feature purification across various SNRs.

**Testing Setup.** We utilize the model averaged over the last 10 checkpoints for evaluation following [23]. During inference, decoding is performed with a left-to-right beam search of width 40 on the Transformer decoder, and following [27], we exploit an off-the-shelf pre-trained GPT-2 language model [28] for beam rescoring. Following prior literature [1, 2], we report word error rate (WER) on LRS3 under both clean and noisy conditions with varying SNR levels. A lower WER indicates better recognition performance, while a lower SNR corresponds to a higher noise level.

### 3.3. Results and Analysis

#### 3.3.1. Influence of the number of bottleneck tokens

The bottleneck tokens serve a key role in our AVBC fusion structure. We thus conduct experiments to evaluate how their quantity influences the model’s final prediction performance under -5dB babble noise. We keep the number of bottleneck tokens to be much smaller than the total latent units per modality, explicitly ensuring only necessary information resides in these bottleneck tokens. Specifically,

**Table 2.** WER (%) comparisons with other competitive methods within different noise levels.

Method	SNR (dB)						Avg.
	clean	15	10	5	0	-5	
EG-Seq2Seq [29]	6.8	3.3	3.9	5.8	12.2	27.3	9.9
Conformer [2]	3.2	3.6	5.4	8.3	14.6	22.3	9.6
V-CAFE [4]	2.9	3.0	4.0	8.4	12.5	19.3	8.4
Joint AVSE-AVSR [11]	2.0	2.4	2.9	4.1	8.0	19.4	6.5
AV-RelScore [12]	2.8	2.9	2.9	3.3	4.8	9.0	4.3
Ours (w/o enh)	2.3	3.1	3.8	4.6	6.7	12.8	5.6
Ours	<b>2.1</b>	<b>2.4</b>	<b>2.6</b>	<b>3.2</b>	<b>4.5</b>	<b>8.5</b>	<b>3.9</b>

**Table 3.** WER (%) comparisons of different methods under clean audio and overlapped speech (SNR=-5dB) inputs, with or without video assistance.

Input Condition	Clean audio		Overlap. speech	
	w/ vid	w/o vid	w/ vid	w/o vid
Unified-Attention [9]	2.4	2.7	11.3	27.4
Our (w/o enh)	2.3	2.5	10.7	25.9
Ours	<b>2.1</b>	<b>2.2</b>	<b>9.6</b>	<b>24.6</b>

we set the number of tokens to 0, 1, 2, 4, 8, and 16 respectively for comparison, where “0” means that the two modalities skip the bottleneck and directly engage in cross-attention. As depicted in Fig. 2, we can observe that the model achieves relatively optimal performance when the number of tokens is set to 4. The results imply that too few tokens may hinder sufficient exchange of essential inter-modal information, while too many could compromise the model’s ability to prioritize only essential content transmission.

### 3.3.2. Effectiveness of the speech enhancement

The audio spectrogram reconstruction within our framework is optimized with two loss functions, *i.e.* the spectrum-based term ( $\mathcal{L}_{\text{recon}}$  in Eq. 2) and the perception-based term ( $\mathcal{L}_{\text{percep}}$  in Eq. 3). We try to assess the effect of each individual loss on final performance. Besides the audio front-end, we also exploit a pre-trained ASR encoder, Whisper [30]<sup>3</sup> medium with fixed parameters, to obtain  $\mathcal{L}_{\text{percep}}$ . Table 1 presents the ablation results under -5dB SNR babble noise, and we find that the combination of these two types of losses can consistently lead to better performance. As our primary objective is AVSR performance not just for clean-sounding audio restoration, the  $\mathcal{L}_{\text{percep}}$  term tends to contribute more to recognition performance by extracting high-level semantic structures of the enhanced audio to improve intelligibility. Compared with the audio front-end, the Whisper can better encourage the enhanced output to preserve rich phonetic and linguistic information that matters for decoding results. But, due to its higher computational overhead, it significantly slows training. Given that our primary goal is robust AVSR – not audio enhancement in isolation – we opt for the audio front-end in this work to maintain training efficiency while still achieving effective gains.

### 3.3.3. Noise robustness evaluation

To investigate the noise robustness of our model against prior competitive baselines, we perform comparative experiments across dif-

ferent acoustic conditions: clean audio and noisy settings with an SNR range of -5 to 15 dB. As shown in Table 2, our proposed method outperforms these advanced noise-robust methods that require explicit noise-reduction masks (*e.g.*, AV-RelScore [12], which incorporates a reliability scoring module to suppress corrupted modal representations) by achieving a lower average WER. Particularly, as SNR level decreases, the performance gap between our method and these baselines widens. Moreover, our full model reduces WER by 1.7% compared to the ablation variant without speech feature enhancement objectives. The results suggest that our method can effectively suppress noisy audio representations without relying on explicit noise mask generation.

### 3.3.4. Experiments on various input conditions

Since cross-modal attention operations are decoupled from the modal encoders, our AVSR framework generalizes to single-modality input sequences, aligning with [9]. To examine the model’s robustness under diverse input conditions, we further conduct evaluations covering clean audio and overlapped speech, each assessed with and without video input. Overlapped speech is generated by randomly selecting a sample from the test set that is distinct from the input audio and overlapping it with the input audio at an SNR of -5dB. During testing, the two distinct speech signals are played simultaneously, while the input video only provides visual cues for the target speech. Notably, the bottleneck tokens within the AVBC still interact with the audio sequence even when video input is disabled. As shown in Table 3, the presence or absence of video input exerts minimal influence on the final performance under clean audio conditions. However, when overlapped speech is used as the audio input, the visual modality becomes crucial for effectively “selecting” the target speech from the mixed speech. Furthermore, our model (without speech enhancement) performs better than the baseline in [9] under overlapped speech scenarios. This advantage likely stems from the bottleneck tokens preserving modality-shared features, which serve as complementary cues for the corrupted audio.

## 4. CONCLUSION

In this paper, we propose a noise-robust AVSR architecture that integrates AVSR with speech enhancement, achieving noise robustness without resorting to explicit noise mask generation. We take advantage of the bottleneck Conformer and audio reconstruction objectives to effectively refine noisy audio representations with video assistance, while preserving speech semantic integrity to facilitate subsequent cross-modal fusion. Experimental results on the LRS3 dataset show superior noise robustness compared to mask-based

<sup>3</sup><https://github.com/openai/whisper>

baseline methods, validating the efficacy of implicit noise suppression enabled by bottleneck-driven cross-modal fusion. Further work will further explore incorporating video reconstruction-based constraints for audio-visual corrupted scenarios.

## 5. REFERENCES

- [1] Triantafyllos Afouras, Joon Son Chung, Andrew W. Senior, Oriol Vinyals, and Andrew Zisserman, “Deep audio-visual speech recognition,” *IEEE TPAMI*, vol. 44, no. 12, pp. 8717–8727, 2018.
- [2] Pingchuan Ma, Stavros Petridis, and Maja Pantic, “End-to-end audio-visual speech recognition with conformers,” in *Proc. ICASSP*, 2021, pp. 7613–7617.
- [3] Maxime Burchi and Radu Timofte, “Audio-visual efficient conformer for robust speech recognition,” in *Proc. WACV*, 2023, pp. 2257–2266.
- [4] Joanna Hong, Minsu Kim, Daehun Yoo, and Yong Man Ro, “Visual context-driven audio feature enhancement for robust end-to-end audio-visual speech recognition,” in *Proc. Interspeech*, 2022, pp. 2838–2842.
- [5] Bowen Shi, Wei-Ning Hsu, Kushal Lakhotia, and Abdelrahman Mohamed, “Learning audio-visual speech representation by masked multimodal cluster prediction,” in *Proc. ICLR*, 2022, pp. 1–24.
- [6] George Sterpu, Christian Saam, and Naomi Harte, “Attention-based audio-visual fusion for robust automatic speech recognition,” in *Proc. ICMI*, 2018, pp. 111–115.
- [7] Liangfa Wei, Jie Zhang, Junfeng Hou, and Lirong Dai, “Attentive fusion enhanced audio-visual encoding for transformer based robust speech recognition,” in *Proc. APSIPA ASC*, 2020, pp. 638–643.
- [8] George Sterpu, Christian Saam, and Naomi Harte, “How to teach dnns to pay attention to the visual modality in speech recognition,” *IEEE/ACM TASLP*, vol. 28, pp. 1052–1064, 2020.
- [9] Jiahong Li, Chenda Li, Yifei Wu, and Yanmin Qian, “Robust audio-visual ASR with unified cross-modal attention,” in *Proc. ICASSP*, 2023, pp. 1–5.
- [10] He Wang, Pengcheng Guo, Pan Zhou, and Lei Xie, “MLCA-AVSR: multi-layer cross attention fusion based audio-visual speech recognition,” in *Proc. ICASSP*, 2024, pp. 8150–8154.
- [11] Jung-Wook Hwang, Jeongkyun Park, Rae-Hong Park, and Hyung-Min Park, “Audio-visual speech recognition based on joint training with audio-visual speech enhancement for robust speech recognition,” *Applied Acoustics*, vol. 211, pp. 109478, 2023.
- [12] Joanna Hong, Minsu Kim, Jeongsoo Choi, and Yong Man Ro, “Watch or listen: Robust audio-visual speech recognition with visual corruption modeling and reliability scoring,” in *Proc. CVPR*, 2023, pp. 18783–18794.
- [13] Arsha Nagrani, Shan Yang, Anurag Arnab, Aren Jansen, Cordelia Schmid, and Chen Sun, “Attention bottlenecks for multimodal fusion,” in *Proc. NeurIPS*, 2021, pp. 14200–14213.
- [14] Triantafyllos Afouras, Joon Son Chung, and Andrew Zisserman, “LRS3-TED: a large-scale dataset for visual speech recognition,” *CoRR*, vol. abs/1809.00496, 2018.
- [15] Kaiming He, Xiangyu Zhang, Shaoqing Ren, and Jian Sun, “Deep residual learning for image recognition,” in *Proc. CVPR*, 2016, pp. 770–778.
- [16] Anmol Gulati, James Qin, Chung-Cheng Chiu, Niki Parmar, Yu Zhang, Jiahui Yu, Wei Han, Shibo Wang, Zhengdong Zhang, Yonghui Wu, and Ruoming Pang, “Conformer: Convolution-augmented transformer for speech recognition,” in *Proc. Interspeech*, 2020, pp. 5036–5040.
- [17] Wenzhe Shi, Jose Caballero, Ferenc Huszar, Johannes Totz, Andrew P. Aitken, Rob Bishop, Daniel Rueckert, and Zehan Wang, “Real-time single image and video super-resolution using an efficient sub-pixel convolutional neural network,” in *Proc. CVPR*, 2016, pp. 1874–1883.
- [18] Justin Johnson, Alexandre Alahi, and Li Fei-Fei, “Perceptual losses for real-time style transfer and super-resolution,” in *Proc. ECCV*, 2016, vol. 9906, pp. 694–711.
- [19] Alex Graves, Santiago Fernández, Faustino J. Gomez, and Jürgen Schmidhuber, “Connectionist temporal classification: labelling unsegmented sequence data with recurrent neural networks,” in *Proc. ICML*, 2006, vol. 148, pp. 369–376.
- [20] Ashish Vaswani, Noam Shazeer, Niki Parmar, Jakob Uszkoreit, Llion Jones, Aidan N. Gomez, Łukasz Kaiser, and Illia Polosukhin, “Attention is all you need,” in *Proc. NeurIPS*, 2017, pp. 5998–6008.
- [21] Takaaki Hori, Shinji Watanabe, and John Hershey, “Joint CTC/attention decoding for end-to-end speech recognition,” in *Proc. ACL*, 2017, pp. 518–529.
- [22] Shinji Watanabe, Takaaki Hori, Suyoun Kim, John R. Hershey, and Tomoki Hayashi, “Hybrid ctc/attention architecture for end-to-end speech recognition,” *IEEE JSTSP*, vol. 11, no. 8, pp. 1240–1253, 2017.
- [23] Pingchuan Ma, Stavros Petridis, and Maja Pantic, “Visual speech recognition for multiple languages in the wild,” *Nat. Mac. Intell.*, vol. 4, no. 11, pp. 930–939, 2022.
- [24] Andrew Varga and Herman J. M. Steeneken, “Assessment for automatic speech recognition: II. NOISEX-92: A database and an experiment to study the effect of additive noise on speech recognition systems,” *Speech Commun.*, vol. 12, no. 3, pp. 247–251, 1993.
- [25] Joon Son Chung and Andrew Zisserman, “Lip reading in the wild,” in *Proc. ACCV*, 2016, vol. 10112, pp. 87–103.
- [26] Ilya Loshchilov and Frank Hutter, “Decoupled weight decay regularization,” in *Proc. ICLR*, 2019, pp. 1–19.
- [27] K. R. Prajwal, Triantafyllos Afouras, and Andrew Zisserman, “Sub-word level lip reading with visual attention,” in *Proc. CVPR*, 2022, pp. 5152–5162.
- [28] Alec Radford, Jeffrey Wu, Rewon Child, David Luan, Dario Amodei, Ilya Sutskever, et al., “Language models are unsupervised multitask learners,” *OpenAI blog*, vol. 1, no. 8, pp. 9, 2019.
- [29] Bo Xu, Cheng Lu, Yandong Guo, and Jacob Wang, “Discriminative multi-modality speech recognition,” in *Proc. CVPR*, 2020, pp. 14421–14430.
- [30] Alec Radford, Jong Wook Kim, Tao Xu, Greg Brockman, Christine McLeavey, and Ilya Sutskever, “Robust speech recognition via large-scale weak supervision,” in *Proc. ICML*, 2023, vol. 202, pp. 28492–28518.